HHS Public Access

Author manuscript

Neural Comput. Author manuscript; available in PMC 2016 September 26.

Published in final edited form as:

Neural Comput. 2016 April ; 28(4): 652–666. doi:10.1162/NECO_a_00818.

Downstream effect of ramping neural activity through synapses with short-term plasticity

Wei Wei[1] and **Xiao-Jing Wang**[1,2]

[1]Center for Neural Science, New York University, New York, NY 10003

[2]NYU-ECNU Joint Institute of Brain and Cognitive Science, NYU Shanghai, Shanghai, China

Abstract

Ramping neuronal activity has been observed in multiple cortical areas correlated with evidence accumulation processes or timing. In this work we investigate the downstream effect of ramping neuronal activity through synapses that display short-term facilitation (STF) or depression (STD). We obtain an analytical result for a synapse driven by deterministic linear ramping input that exhibits pure STF or STD, and investigate the general case when both STF and STD exist numerically. In neural circuits, the ramping inputs usually have strong fluctuation and each downstream neuron receives converging inputs from many presynaptic neurons. We show that the analytical deterministic solution gives an accurate description of the averaging synaptic activation that a postsynaptic neuron receives in a neural circuit, even when the fluctuation in ramping input is strong. Therefore our work provides insights on the impact of ramping neuronal activity on downstream neurons through synapses displaying short-term plasticity. Specifically, activation of a synapse with STF shows a sublinear increase with time and is insensitive to the slopes of ramping inputs during the initial period, followed by a linear ramping similar to a synapse without STF. Activation of a synapse with STD, on the other hand, develops a local maximum before reaching a steady state, which is independent of the slope of ramping input. For a synapse displaying both STF and STD, increase of the depression time constant from a value much smaller than the facilitation time constant τ_F to a value much larger than τ_F leads to a transition from facilitation domination to depression domination. By utilizing STD in the corticostriatal synapses, our work provides an understanding of the saturation of striatal activity as observed for monkeys performing evidence accumulation. Our work also predicts that in the fixed duration version of motion discrimination tasks the stationary state of neuronal activity downstream to the decision circuit will be independent of the motion coherences.

Keywords

ramping neuronal activity; short-term facilitation; short-term depression

1 Introduction

Ramping neuronal activity has been observed in different cortical and subcortical areas, such as lateral intraparietal cortex, frontal eye field, superior colliculus, thalamus, presupplementary and supplementary motor areas, etc., and provides a neuronal implementation of the evidence accumulation process during perceptual decision making

(Wang, 2002; Gold and Shadlen, 2007; Wang, 2008) and timing (Komura et al., 2001; Reutimann et al., 2004; Mita et al., 2009; Simen et al., 2011; Merchant et al., 2013). A simple mathematical model for the ramping neuronal activities is the drift-diffusion model (Hanes and Schall, 1996; Huk and Shadlen, 2005; Ratcliff et al., 2003). Recently, neurons in the caudate nucleus (the eye movement part of the striatum) have been observed to show a ramping activity followed by a saturation before saccade initiation (Ding and Gold, 2010). The striatum receives direct projections from cortical areas that display ramping neuronal activity. The origin of the saturation of ramping activity in the striatum is not well understood yet.

Short-term plasticity (STP) is a common feature of cortical synapses, and both short-term facilitation (STF) and depression (STD) have been observed in the cortex (Abbott and Regehr, 2004; Morrison et al., 2008). In the phenomenological model of STP, depression is attributed to a decrease of vesicle availability, while facilitation is attributed to an increase of vesicle release probability (Tsodyks and Markram, 1997; Tsodyks et al., 1998; Fuhrmann et al., 2002; Hempel et al., 2000). For simplicity in theoretical understanding of the role of synaptic plasticity, pure depression or facilitation was often considered, although in general both depression and facilitation coexist in a synapse. In both experimental and theoretical investigations, presynaptic input with a constant rate is usually applied. The saturation of striatal ramping during evidence accumulation has been related to STD in the corticostriatal synapses (Wei et al., 2015). In this work, we analytically characterized the downstream effect of synapses displaying STF or STD driven by fluctuating ramping presynaptic inputs described by the drift-diffusion model. We also investigated the general case when both STF and STD coexist in a synapse numerically.

2 Phenomenological model for STP

In the phenomenological model for STP, the activity of a synapse with pure STF is described as following,

$$\frac{dF}{dt}=\alpha(1-F)\sum_j \delta(t-t^j)-\frac{F}{\tau_F} \quad (1)$$

$$\frac{ds}{dt}=F\sum_j \delta(t-t^j)-\frac{s}{\tau_a} \quad (2)$$

where t^j is the time of the jth presynaptic input spike, F represents the vesicle release probability, and s is the gating variable. At the arriving a presynaptic spike, F first increases with an amount $\alpha(1-F)$, and then decays with a time constant τ_F during the intervals of input spikes. The gating variable s is then updated following the update of F, with an increment of F. The conductance to a postsynaptic neuron is given by the product of the gating variable s and a constant synaptic efficacy.

The presynaptic spike train in Eq. (1–2) represents the instantaneous input firing rate $r(t)$, i.e., $r(t) \simeq \Sigma_j \delta(t - t^j)$. Here we are interested with the case when $r(t)$ describes a ramping input rate as observed for cortical neurons in multiple brain areas. The ramping input rate $r(t)$ is well described by the classical drift-diffusion model,

$$\tau \frac{dr}{dt} = \mu + \sigma \sqrt{\tau} \eta(t) \quad (3)$$

where τ is the time constant for the drift-diffusion process, μ is the drift term, $\eta(t)$ is a Gaussian white noise satisfying $\langle \eta(t) \rangle = 0$ and $\langle \eta(t)\ \eta(t') \rangle = \delta(t - t')$, and σ is the noise strength. We will take $\tau = 10$ ms, but all the results will not depend on the exact value of τ. The synaptic dynamics are given by the following equations,

$$\frac{dF}{dt} = \alpha(1 - F) r(t) - \frac{F}{\tau_F} \quad (4)$$

$$\frac{ds}{dt} = F r(t) - \frac{s}{\tau_a} \quad (5)$$

We will use $\tau_a = 2$ ms, $\tau_F = 400$ ms, and $\alpha = 0.25$. The value for τ_a is characteristic of the decay time constant for AMPAergic synapses. Different values of τ_F and α (with $\tau_F \gg \tau_a$) will not qualitatively change the behavior of the phenomenological model.

For a synapse with pure STD, the synaptic dynamics are described as following,

$$\frac{dD}{dt} = -pD \sum_j \delta(t - t^j) + \frac{1 - D}{\tau_D} \quad (6)$$

$$\frac{ds}{dt} = pD \sum_j \delta(t - t^j) - \frac{s}{\tau_a} \quad (7)$$

where p is a constant vesicle release probability, D represents the fraction of available vesicles. At the arriving of a presynaptic spike, D is first reduced by an amount pD, and then recovered with a time constant τ_D during the intervals of input spikes. The gating variable s is then updated following the update of D, with an increment of pD.

Replacing the presynaptic spike train by the instantaneous input rate $r(t)$ described by Eq. (3), we have the following equations,

$$\frac{dD}{dt}=-pr(t)D+\frac{1-D}{\tau_D} \quad (8)$$

$$\frac{ds}{dt}=pr(t)D-\frac{s}{\tau_a} \quad (9)$$

We will use $p = 0.45$, $\tau_D = 600$ ms. Different values of p and τ_D (with $\tau_D \gg \tau_a$) will not qualitatively change the behavior of the phenomenological model.

We will first study a deterministic linear ramping input ($\sigma = 0$ case) and then consider a general fluctuating ramping input described by the drift-diffusion model. The initial values of F, D and s at $t = 0$ are denoted as F_0, D_0 and s_0. We will use $F_0 = 0$, $D_0 = 1$, and $s_0 = 0$ if not stated otherwise.

3 Deterministic linear ramping input

3.1 Synapse with STF

When $\sigma = 0$ in Eq. (3), the input rate ramps up linearly with time, i.e., $r = kt$, where $k \equiv \mu/\tau$ is the slope of ramping. Eq. (4–5) can be solved analytically,

$$F=1-\exp\left(-\frac{1}{2}\alpha k t^2-\frac{t}{\tau_F}\right)\left(1-F_0-\frac{1}{\tau_F}\sqrt{\frac{2}{\alpha k}}\mathcal{F}\left(\frac{1}{\tau_F\sqrt{2\alpha k}}\right)\right)-\frac{1}{\tau_F}\sqrt{\frac{2}{\alpha k}}\mathcal{F}\left(\sqrt{\frac{\alpha k}{2}}t+\frac{1}{\tau_F\sqrt{2\alpha k}}\right)$$

(10)

$$s \simeq k\tau_a F t \quad (11)$$

where $\mathcal{F}(x)$ is the Dawson's integral (Abramowitz and Stegun, 1970) as defined in the Appendix.

In Fig. 1, the synaptic dynamics for ramping input with two different slopes and constant input (Fig. 1A) are illustrated and are compared with the control case when there is no STP (Fig. 1B). The activities of F and s for a synapse with STF are shown in Fig. 1C–D. When t is large, we have

$$F \simeq 1-\frac{1}{\alpha\tau_F kt+1} \to 1 \quad (12)$$

$$s \simeq \frac{\alpha\tau_a\tau_F k^2t^2}{\alpha\tau_F kt+1} \to \tau_a kt \quad (13)$$

Therefore when t is large, the facilitation factor F will saturate hyperbolically for a ramping input, while for a constant input it will reach its stationary state exponentially (Fig. 1C and also see the Appendix). The gating variable s will increase sublinearly at the initial period (gray region in Fig. 1D, with width τ_F), then followed by a linear increase similar to the control case (Fig. 1B). Note that for a constant input rate, s will saturate when t is large in the time scale τ_F for a synapse with STF (Fig. 1D, black curve), while in the control case s will saturate to its steady state in the much shorter time scale τ_a (Fig. 1B, black curve).

3.2 Synapse with STD

For $r = kt$ and $\sigma = 0$, from Eq. (8–9) we have

$$D=\frac{1}{\tau_D}\sqrt{\frac{2}{kp}}\mathscr{F}\left(\sqrt{\frac{kp}{2}}t+\frac{1}{\tau_D\sqrt{2kp}}\right)+\left(D_0-\frac{1}{\tau_D}\sqrt{\frac{2}{kp}}\mathscr{F}\left(\frac{1}{\tau_D\sqrt{2kp}}\right)\right)\exp\left(-\left(\frac{1}{2}pkt^2+\frac{t}{\tau_D}\right)\right)$$

(14)

$$s \simeq pk\tau_a Dt \quad (15)$$

When t is large,

$$D \simeq \frac{1}{\tau_D}\sqrt{\frac{2}{kp}}\frac{1}{2(\sqrt{\frac{kp}{2}}t+\frac{1}{\tau_D\sqrt{2kp}})}=\frac{1}{kp\tau_D t+1}\to\frac{1}{kp\tau_D t} \quad (16)$$

$$s \to \frac{\tau_a}{\tau_D} \quad (17)$$

We see that for the ramping input, D decays hyperbolically for large t, which is slower than that for a constant input rate which decays exponentially to its steady state (Fig. 1E). The gating variable s will reach a steady state, which is independent with the ramping slope k and release probability p (Fig. 1D). Note that the steady state for a ramping input is the same as that for a constant input when the constant rate is large enough, as given in the Appendix.

Before reaching its steady state, the gating variable s for a synapse with STD will develop a maximum when receiving ramping input (Fig. 1F). Although the steady state of s is independent of the ramping slope k and the release probability p, the maximal value of s depends on both k and p. For small t and applying Eq. (30),

$$D \simeq \frac{1}{\tau_D}\sqrt{\frac{2}{kp}}\left(\sqrt{\frac{kp}{2}}t+\frac{1}{\tau_D\sqrt{2kp}}\right)+(1-\frac{1}{kp\tau_D^2})(1-\frac{t}{\tau_D}-\frac{1}{2}kpt^2)$$
$$=1+\frac{t}{kp\tau_D^3}-\frac{1}{2}kpt^2\left(1-\frac{1}{kp\tau_D^2}\right) \quad (18)$$

where $\frac{1}{kp\tau_D^2}(\sim 0.1)$ is small, so we have

$$D \simeq 1-\frac{1}{2}kpt^2 \quad (19)$$

By comparing Eq. (19) with Eq. (36) in the Appendix, we see the different small time behaviors of D for ramping and constant input rates (Figure 1E). Therefore, when t is small (but $t > \tau_a$),

$$s \simeq pk\tau_a t(1-\frac{1}{2}pkt^2) \quad (20)$$

which has a maximal value at time t_{max} given by

$$t_{max}=\sqrt{\frac{2}{3}}\frac{1}{\sqrt{pk}} \quad (21)$$

$$s_{max}=\sqrt{\frac{8}{27}}\sqrt{pk}\,\tau_a \quad (22)$$

Fig. 2A and 2B compares the approximate and real values of t_{max} and s_{max} as a function of k, respectively. We see that Eq. (21–22) provide qualitative information about the location and value of the maximum of s: A ramping input with a higher slope k will have a larger maximum developed within a shorter time.

3.3 Synapse with both STF and STD

In general, there are both STF and STD coexisting in a synapse, with the dynamics described by (Tsodyks et al., 1998; Hempel et al., 2000; Lindner et al., 2009)

$$\frac{dF}{dt}=\alpha r(t)(1-F)-\frac{F}{\tau_F} \quad (23)$$

$$\frac{dD}{dt}=-r(t)FD+\frac{1-D}{\tau_D} \quad (24)$$

$$\frac{ds}{dt}=r(t)FD-\frac{s}{\tau_a} \quad (25)$$

For a deterministic linear input rate, $r = kt$, the solution of Eq. (23) is given by Eq. (10). Since τ_a is much smaller than τ_F and τ_D, Eq. (25) is simplified to

$$s \simeq k\tau_a FDt \quad (26)$$

Eq. (24), however, can not be solved analytically. For large t, $F \to 1$ (Eq. 12). When $\tau_F \ll \tau_D$, the synapse is depression-dominated, and $D \to \frac{1}{k\tau_D t}$ (Eq. 16, replacing p with $F \to 1$). Therefore when $\tau_F \ll \tau_D$, we have

$$s \to \frac{\tau_a}{\tau_D} \quad (27)$$

the same long time limit as that for a synapse with pure STD.

We solve Eq. (24) numerically and show the time evolution of facilitation factor F, depression factor D, and gating variable s in Fig. 3 for different model parameters. The top row of Fig. 3 shows the dependence of synaptic dynamics on a. Note that here we illustrates a depression-dominated synapse. We see that with a larger a, the increase of F and the decrease of D with time become faster, and s has a larger maximum and reaches its maximum faster (A1–A3 in Fig. 3). Modulating a does not qualitatively changes the synaptic dynamics (the same conclusion still holds for a facilitation-dominated synapse). We also see that the long time limit of s does not depend on a (A3 in Fig. 3), as Eq. (27) suggests.

The dependence of synaptic dynamics on the facilitation time constants τ_F for a facilitation-dominated synapse is shown in the middle row of Fig. 3. With a larger τ_F, the increase of F and s, and the decrease of D become faster (B1–B3 in Fig. 3). When $\tau_F \gg \tau_D$, D and s become insensitive to the value of τ_F (see the blue and green curves in B2 and B3, Fig. 3). We see that after a rapid increase period, the activation level of the gating variable s for a

facilitation-dominated synapse increases much slower than that for a synapse with pure STF (compare the blue curves in Fig. 1D and in B3, Fig. 3). For a depression-dominated synapse, D and s only weakly depend on τ_F (data not shown). The bottom row in Fig. 3 shows the dependence of synaptic dynamics on the depression time constants τ_D. We see that the facilitation factor F is independent of τ_D (C1 in Fig. 3) by design (Eq. 23), while the depression factor D decreases faster with a larger τ_D (C2 in Fig. 3). Interestingly, the gating variable s shows a transition from facilitation domination to depression domination when τ_D increases from a value much smaller than τ_F to a value much larger than τ_F (black and green curves in C3, Fig. 3). Therefore, the interaction of F and D determines whether the synapse is facilitation- or depression-dominated.

4 Fluctuating ramping input

We now consider the case when the ramping input is noisy and is described by Eq. (3), as cortical neurons downstream to a decision circuit will receive. Each downstream neuron receives a summation of inputs from many presynaptic neurons. Since the synaptic efficacy scale with the number of presynaptic neurons, the conductance to a downstream neuron is given by the average gating variables, denoted as $\langle s \rangle$. The angular bracket represents averaging over presynaptic neuronal populations, which is implemented in simulations by averaging different realizations of the noise. The upper row of Fig. 4 shows 10 different realizations of $x(t)$ (A), gating variable s for synapses with pure STF (B) and with pure STD (C), and the corresponding averaging values over 300 realizations for $\mu = 0.5$ Hz (i.e., $k = 50$ sec^{-2}).

Fig. 4 (lower row) shows the results for $\sigma = 0$, 0.5, and 1 Hz when $\mu = 0.5$ Hz. As one expects, the average ramping input $x(t)$ follows the deterministic trajectory (Fig. 4D). Since Eq. (4) and (8) can not be solved analytically due to the interaction term between $x(t)$ and F or D, we hope the deterministic results obtained in the preceding section can give a good approximation to the average synaptic activation in the low noise regime, i.e., when σ is small. From Fig. 4E and 4F, we see that the deterministic results give a very accurate approximation ($R^2 = 0.999$ and 0.993 in Fig. 4E for STF, $R^2 = 0.996$ and 0.944 in Fig. 4F, when $\sigma = 0.5$ and 1 sec^{-1}, respectively), even when the noise level is two times the drift term. Therefore, the theoretical results for deterministic ramping input provide a good description for the conductance of downstream neurons receiving ramping inputs described by the drift-diffusion model.

5 Discussion

We investigated the downstream effect of ramping neuronal activity through synapses showing STP. We first derived analytical results for deterministic linear ramping input through synapses displaying pure STF or STD, and showed the different synaptic dynamics in contrast to a steady input rate. We obtained a simple approximation for the maximal value of the activation level and the time taken to reach the maximum for a synapse with pure STD. For the general case when a synapse shows both STF and STD effects, we found that it behaves as a synapse with pure STD when the facilitation time constant τ_F is much smaller than the depression time constant τ_D. We further investigated the dependence of synaptic

dynamics on model parameters numerically in the general case. We found a transition from facilitation domination to depression domination when τ_D increases from a value much smaller than τ_F to a value much larger than τ_F. A downstream neuron will receive an averaged input from the presynaptic population. We then showed that the averaged synaptic activation level to the downstream neuron is well described by the deterministic solution even when the fluctuation of the ramping input is strong. These results provide insights for downstream impacts of ramping neuronal activity through synapses showing STP.

Cortical areas showing ramping neuronal activity project to other cortical areas and also subcortical areas such as the striatum, thalamus, and superior colliculus. The striatal activity has been observed to ramp up followed by saturation during evidence accumulation when monkeys performed perceptual decision making (Ding and Gold, 2010). Our work showed that this observation could be explained by utilizing STD in the corticostriatal synaptic projection. A direct measurement of EPSP/EPSC for synapses receiving ramping input is not available yet. Our results could be easily tested by intracellular recording of slices with NMDA receptors blocked and receiving external synthesized ramping input with the slope adjustable. For synapses with STF, our results showed that the activation of gating variable is slower and less sensitive to the ramping slope at the early stage than the control case without STP, followed by the same linear increase as in the control case since $F \to 1$ for large t. For synapses with STD, the ramping slope is only encoded at the initial period of evidence accumulation and the steady state is insensitive to it. This predication can be tested in the fixation time version of perceptual decision making tasks. Therefore we showed the differential properties of synapses with STF and STD in encoding the slope of ramping activity, which represents the bias of stimulus in making decisions.

One future direction is to include the intrinsic synaptic noise in the deterministic model for STP and investigate its influence when the synapse is driven by fluctuating ramping input. Depressing synapses with intrinsic noise receiving a Poisson input with constant rate has been studied (Rosenbaum et al., 2012, 2013). Synapses displaying STD and stochastic vesicle dynamics were shown to behave as a frequency-dependent filter in signal transmission (Matveev and Wang, 2000; Rosenbaum et al., 2012), in contrast to the broadband signal transmission for deterministic synapses (Lindner et al., 2009), and also influence the transfer of neuronal correlations (Rosenbaum et al., 2013). Extension of our work to include intrinsic synaptic noise will provide further insights about the downstream impact of ramping neuronal activity during perceptual decision making and timing.

Acknowledgments

This work was supported by a Swartz Foundation Fellowship (W.W.), and the National Institutes of Health Grants R01 MH062349 (X.-J. W).

References

Abbott LF, Regehr WG. Synaptic computation. Nature. 2004; 431:796–803. [PubMed: 15483601]

Abramowitz, M.; Stegun, I. Handbook of Mathematical Functions with Formulas, Graphs, and Mathematical Tables. Dover Publications; New York: 1970.

Ding L, Gold JI. Caudate encodes multiple computations for perceptual decisions. J Neurosci. 2010; 30:15747–15759. [PubMed: 21106814]

Fuhrmann G, Segev I, Markram H, Tsodyks M. Coding of temporal information by activity-dependent synapses. J Neurophysiol. 2002; 87(1):140–148. [PubMed: 11784736]

Gold JI, Shadlen MN. The neural basis of decision making. Annu Rev Neurosci. 2007; 30:535–574. [PubMed: 17600525]

Hanes DP, Schall JD. Neural control of voluntary movement initiation. Science. 1996; 274:427–430. [PubMed: 8832893]

Hempel CM, Hartman KH, Wang XJ, Turrigiano GG, Nelson SB. Multiple forms of short-term plasticity at excitatory synapses in rat medial prefrontal cortex. J Neurophysiol. 2000; 83:3031–3041. [PubMed: 10805698]

Huk AC, Shadlen MN. Neural activity in macaque parietal cortex re-flects temporal integration of visual motion signals during perceptual decision making. J Neurosci. 2005; 25:10420–10436. [PubMed: 16280581]

Komura Y, Tamura R, Uwano T, Nishijo H, Kaga K, Ono T. Retrospective and prospective coding for predicted reward in the sensory thalamus. Nature. 2001; 412:546–549. [PubMed: 11484055]

Lindner B, Gangloff D, Longtin A, Lewis JE. Broadband coding with dynamic synapses. J Neurosci. 2009; 29:2076–2088. [PubMed: 19228961]

Matveev V, Wang XJ. Differential short-term synaptic plasticity and transmission of complex spike trains: to depress or to facilitate? Cereb Cortex. 2000; 10:1143–1153. [PubMed: 11053234]

Merchant H, Harrington DL, Meck WH. Neural basis of the perception and estimation of time. Annu Rev Neurosci. 2013; 36:313–336. [PubMed: 23725000]

Mita A, Mushiake H, Shima K, Matsuzaka Y, Tanji J. Interval time coding by neurons in the presupplementary and supplementary motor areas. Nat Neurosci. 2009; 12:502–507. [PubMed: 19252498]

Morrison A, Diesmann M, Gerstner W. Phenomenological models of synaptic plasticity based on spike timing. Biol Cybern. 2008; 98:459–478. [PubMed: 18491160]

Ratcliff R, Cherian A, Segraves M. A comparison of macaque behavior and superior colliculus neuronal activity to predictions from models of two-choice decisions. J Neurophysiol. 2003; 90:1392–1407. [PubMed: 12761282]

Reutimann J, Yakovlev V, Fusi S, Senn W. Climbing neuronal activity as an event-based cortical representation of time. J Neurosci. 2004; 24:3295–3303. [PubMed: 15056709]

Rosenbaum R, Rubin J, Doiron B. Short term synaptic depression imposes a frequency dependent filter on synaptic information transfer. PLoS Comput Biol. 2012; 8:e1002557. [PubMed: 22737062]

Rosenbaum R, Rubin JE, Doiron B. Short-term synaptic depression and stochastic vesicle dynamics reduce and shape neuronal correlations. J Neurophysiol. 2013; 109:475–484. [PubMed: 23114215]

Simen P, Balci F, de Souza L, Cohen JD, Holmes P. A model of interval timing by neural integration. J Neurosci. 2011; 31:9238–9253. [PubMed: 21697374]

Tsodyks M, Pawelzik K, Markram H. Neural networks with dynamic synapses. Neural Comput. 1998; 10:821–835. [PubMed: 9573407]

Tsodyks MV, Markram H. The neural code between neocortical pyramidal neurons depends on neurotransmitter release probability. Proc Natl Acad Sci USA. 1997; 94:719–723. [PubMed: 9012851]

Wang XJ. Probabilistic decision making by slow reverberation in cortical circuits. Neuron. 2002; 36:955–968. [PubMed: 12467598]

Wang XJ. Decision making in recurrent neuronal circuits. Neuron. 2008; 60:215–234. [PubMed: 18957215]

Wei W, Rubin JE, Wang XJ. Role of the indirect pathway of the basal ganglia in perceptual decision making. J Neurosci. 2015; 35:4052–4064. [PubMed: 25740532]

Appendix

The Dawson's integral $\mathcal{F}(x)$ is defined as (Abramowitz and Stegun, 1970)

$$\mathcal{F}(x)=e^{-x^2}\int_0^x e^{y^2}\,dy \quad (28)$$

$\mathcal{F}(x)$ has the following asymptotic expansion

$$\mathcal{F}(x)\simeq\frac{1}{2x}+\frac{1}{4x^3}+\dots \quad (29)$$

when x is large, and the series expansion

$$\mathcal{F}(x)\simeq x-\frac{2}{3}x^3+\frac{4}{15}x^5\dots \quad (30)$$

when x is small (Abramowitz and Stegun, 1970).

For comparison, we present here results for a constant input rate, $r(t) \equiv r$. For a synapse with pure STF, the solutions for Eq. (4–5) are given by

$$F=\frac{\alpha r\tau_F}{1+\alpha r\tau_F}+\left(F_0-\frac{\alpha r\tau_F}{1+\alpha r\tau_F}\right)\exp\left(-(1+\alpha r\tau_F)\frac{t}{\tau_F}\right) \quad (31)$$

$$s=r\tau_a F \quad (32)$$

For large t,

$$s\to\frac{\alpha r^2\tau_a\tau_F}{1+\alpha r\tau_F} \quad (33)$$

For a synapse with pure STD, the solutions of Eq. (8–9) are given by

$$D=\frac{1}{1+\tau_D pr}+\left(D_0-\frac{1}{1+\tau_D pr}\right)\exp\left(-(1+\tau_D pr)\frac{t}{\tau_D}\right) \quad (34)$$

$$s=pr\tau_a D \quad (35)$$

When t is small (but larger than τ_a),

$$D \simeq 1-prt \quad (36)$$

When t is large, D and s reach their steady states,

$$D \to \frac{1}{1+\tau_D pr} \quad (37)$$

$$s \to \frac{pr\tau_a}{1+\tau_D pr} \quad (38)$$

When $\tau_D pr \gg 1$, i.e., $r \gg \frac{1}{\tau_D p} = \frac{1}{0.6*0.45} = 3.7$ Hz, this steady state of s is reduced to

$$s \to \frac{\tau_a}{\tau_D} \quad (39)$$

which is independent of the constant input rate r and release probability p, and has the same expression as the steady state for a deterministic linear ramping input (Eq. 17).

As a control case, we consider a synapse without STP. Taking $F = 1$ in Eq. (5), then the activation of the synapse is given by

$$s = k\tau_a t + k\tau_a^2(e^{-t/\tau_a}-1) + s_0 e^{-t/\tau_a} \quad (40)$$

for a ramping input rate $r = kt$, and

$$s = r\tau_a(1-e^{-t/\tau_a}) + s_0 e^{-t/\tau_a} \quad (41)$$

for a constant input rate r.

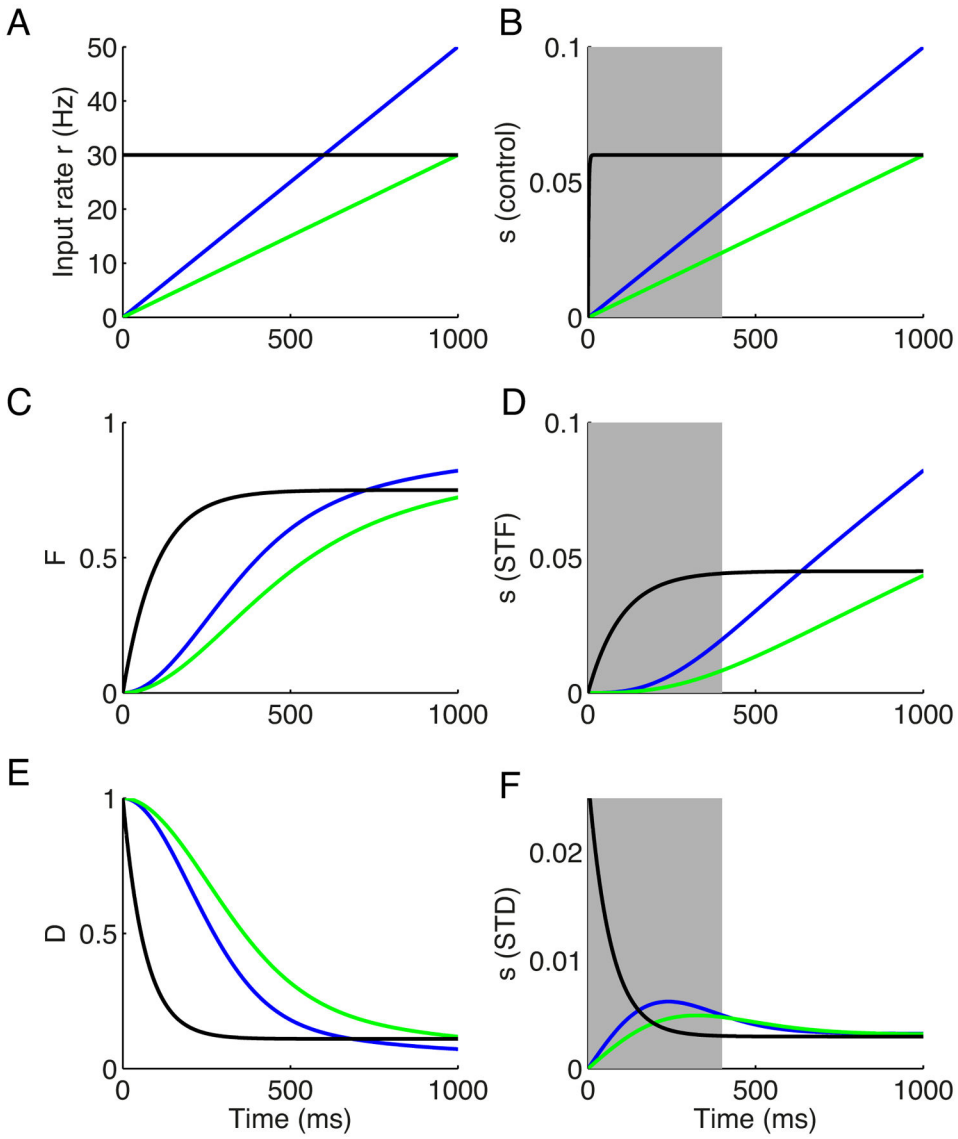

Figure 1.

Activation level of a synapse with pure STF or STD. A, The input rate ramps up linearly, with slope $k = 30$ (green) and 50 (blue) (in sec^{-2}). The black curve represents a constant input with rate 30 Hz. B, The activation level of the gating variable s in the control case when there is no STP. C,D, The facilitation factor F (C) and the activation level s (D) for a synapse with pure STF. E,F, The depression factor D (E) and activation level s (F) for a synapse with pure STD. The gray shaded areas (with width τ_F) highlight the different activity of s for a synapse with and without STP. Parameters used: $\tau_a = 2$ ms, $\tau_F = 400$ ms, $\alpha = 0.25$, $\tau_D = 600$ ms, $p = 0.45$.

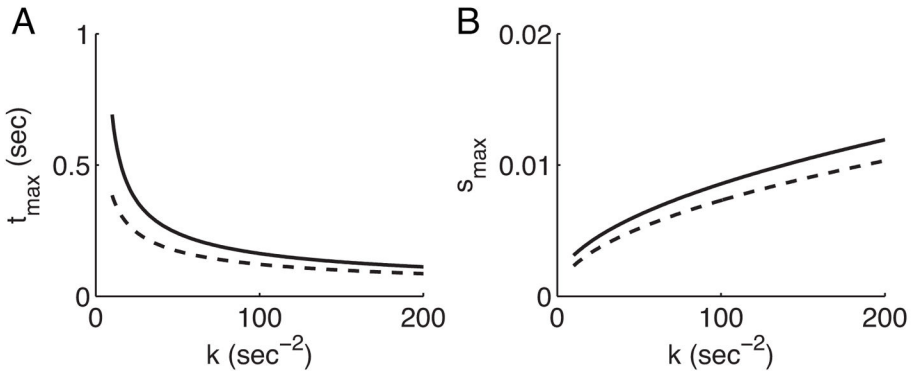

Figure 2.

The maximal activation level and the time for reaching the maximum for a synapse with pure STD as a function of ramping slope. A, The time for reaching the maximum of s as a function of the ramping slope k. B, The maximal value of s as a function of the ramping slope k. The dashed lines in A and B are approximations from Eq. (21) and (22), respectively.

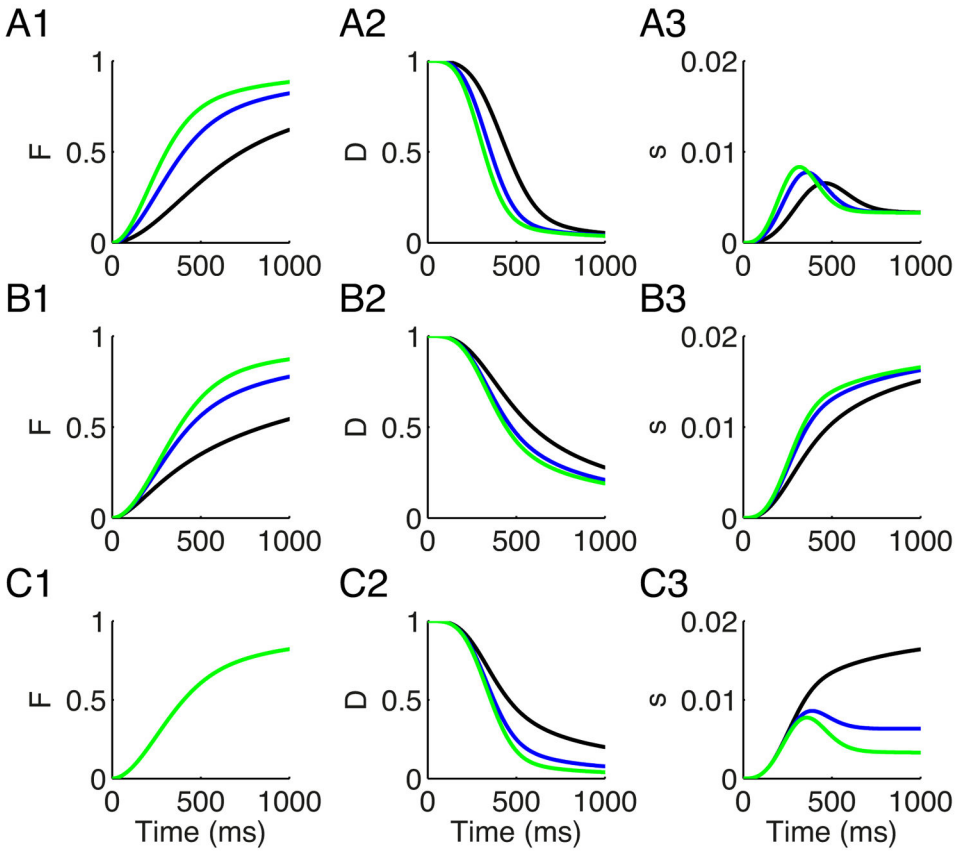

Figure 3.

Activation level of a synapse with both STF and STD. A1–A3, The time evolution of facilitating factor F (A1), depressing factor D (A2), and gating variable s (A3) for different a (green, 0.1; blue, 0.25; black, 0.4). B1–B3, The time evolution of F (B1), D (B2), and s (B3) for different τ_F (green, 100 ms; blue, 300 ms; black, 600 ms). C1–C3, The time evolution of F (C1), D (C2), and s (C3) for different τ_D (green, 100 ms; blue, 300 ms; black, 600 ms). Parameters used: $k = 50$ sec^{-2}, $\tau_a = 2$ ms. In A1–A3, $\tau_F = 400$ ms, $\tau_D = 600$ ms. In B1–B3, $\tau_D = 100$ ms, $a = 0.25$. In C1–C3, $\tau_F = 400$ ms, $a = 0.25$.

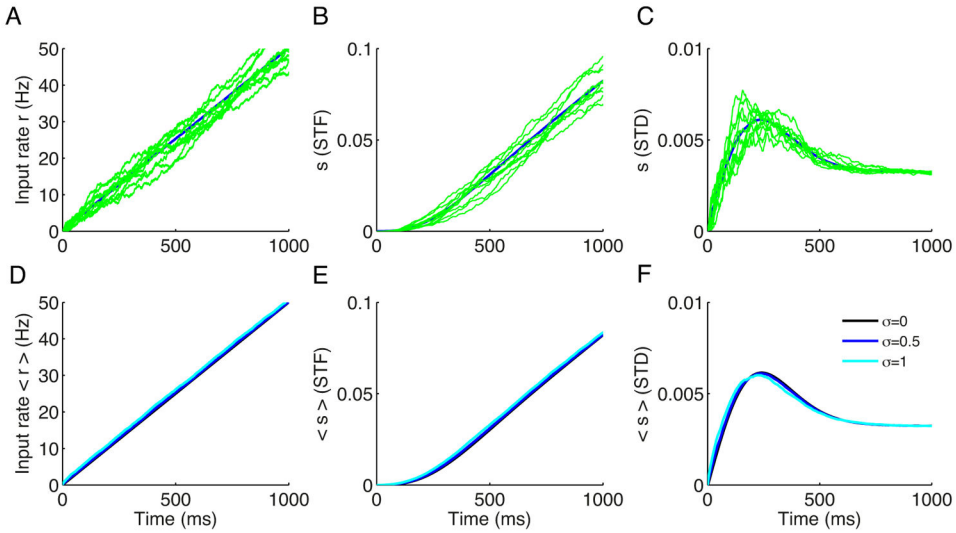

Figure 4.

Synaptic activation of a downstream neuron that receives inputs from a population of presynaptic neurons showing ramping activity. A–C, Fluctuating ramping input described by the drift-diffusion model (A), the activation level s for synapses with pure STF (B), and for synapses with pure STD (C). Blue, the average activity of $r(t)$ (A) and s (B–C) over 300 realizations. Green: illustrated trajectories for 10 realizations. In A–C, $\mu = 0.5$ sec $^{-1}$ (i.e., $k = 50$ sec^{-2}) and $\sigma = 0.5$ sec^{-1}. D–F, Ensemble averaged ramping inputs $\langle r \rangle$ (D), activation level $\langle s \rangle = \frac{1}{N}\sum_i s_i$ for synapses with pure STF (E), and pure STD (F) for different noise levels with $\mu = 0.5$, $\sigma = 0$, 0.5, and 1 (in sec^{-1}). N is the size of presynaptic population.